Thermodynamics of Metal Ion Binding and Denaturation of a Calcium Binding Protein from *Entamoeba histolytica*†

B. Gopal,‡ C. P. Swaminathan,‡ Sudha Bhattacharya,§ Alok Bhattacharya,|| M. R. N. Murthy,*,‡ and A. Surolia‡

Molecular Biophysics Unit, Indian Institute of Science, Bangalore 560 012, India, School of Environmental Sciences, Jawaharlal Nehru University, New Delhi 110 067, India, and School of Life Sciences, Jawaharlal Nehru University, New Delhi 110 067, India

Received February 3, 1997; Revised Manuscript Received May 15, 1997⊗

ABSTRACT: The thermodynamics of the binding of calcium and magnesium ions to a calcium binding protein from *Entamoeba histolytica* was investigated by isothermal titration calorimetry (ITC) in 20 mM MOPS buffer (pH 7.0) at 20 °C. Enthalpy titration curves of calcium show the presence of four Ca^{2+} binding sites. There exist two low-affinity sites for Ca^{2+}, both of which are exothermic in nature and with positive cooperative interaction between them. Two other high affinity sites for Ca^{2+} exist of which one is endothermic and the other exothermic, again with positive cooperative interaction. The binding constants for Ca^{2+} at the four sites have been verified by a competitive binding assay, where CaBP competes with a chromophoric chelator 5, 5′-Br_2 BAPTA to bind Ca^{2+} and a Ca^{2+} titration employing intrinsic tyrosine fluorescence of the protein. The enthalpy of titration of magnesium in the absence of calcium is single site and endothermic in nature. In the case of the titrations performed using protein presaturated with magnesium, the amount of heat produced is altered. Further, the interaction between the high-affinity sites changes to negative cooperativity. No exchange of heat was observed throughout the addition of magnesium in the presence of 1 mM calcium. Titrations performed on a cleaved peptide comprising the N-terminus and the central linker show the existence of two Ca^{2+} specific sites. These results indicate that this CaBP has one high-affinity Ca-Mg site, one high-affinity Ca-specific site, and two low-affinity Ca-specific sites. The thermodynamic parameters of the binding of these metal ions were used to elucidate the energetics at the individual site(s) and the interactions involved therein at various concentrations of the denaturant, guanidine hydrochloride, ranging from 0.05 to 6.5 M. Unfolding of the protein was also monitored by titration calorimetry as a function of the concentration of the denaturant. These data show that at a GdnHCl concentration of 0.25 M the binding affinity for the Mg^{2+} ion is lost and there are only two sites which can bind to Ca^{2+}, with substantial loss of cooperativity. At concentrations beyond 2.5 M GdnHCl, at which the unfolding of the tertiary structure of this protein is observed by near UV CD spectroscopy, the binding of Ca^{2+} ions is lost. We thus show that the domain containing the two low-affinity sites is the first to unfold in the presence of GdnHCl. Control experiments with change in ionic strength by addition of KCl in the range 0.25−1 M show the existence of four sites with altered ion binding parameters.

Calcium has been shown to regulate the pathogenesis of *Entamoeba histolytica* based on the ability of the calcium antagonists to block the cytopathic function of amoeba and the release of the secretary collagenase (Ravdin et al., 1985; Munoz et al., 1991). In order to elucidate the mechanisms of Ca^{2+} signaling in *E. histolytica*,[1] a CaBP was isolated and the corresponding sequence was cloned and expressed in *E. coli* (Prasad et al., 1993).

E. histolytica CaBP exists as a monomer (molecular mass = 14.7 kDa). On the basis of sequence comparisons with other proteins in the EF hand superfamily, this CaBP is proposed to have a two domain structure, separated by a central linker. The recombinant protein has four sites strongly resembling in sequence to other EF hand Ca^{2+} binding motifs (Figure 1). However, the overall amino acid sequence identity of *E. histolytica* CaBP to other CaBP's is not very high. In the case of Calmodulin, a trigger CaBP (Wang, 1985; Drabikowski et al., 1982), it has been shown that it has two high-affinity Ca^{2+}-Mg^{2+} sites and two low-affinity Ca^{2+}-specific sites. Troponin C, another trigger CaBP, similar in structure to Calmodulin, has been reported to have sites which are classified as two high-affinity Ca-Mg sites, two low affinity Ca-specific sites, and around two Mg-specific sites (Imaizumi et al., 1989), while parvalbumin, a buffer CaBP, has two high-affinity Ca-Mg sites.

In the present study, microcalorimetric titrations were performed at 20 °C with calcium, magnesium, and competitive binding experiments with calcium titrated with a magnesium saturated protein and *vice versa*. The results

† Supported by the grants from the Department of Science and Technology, Government of India to M.R.N. and A.S.

* Corresponding author: Molecular Biophysics Unit, Indian Institute of Science, Bangalore 560 012. Email: mrn@mbu.iisc.ernet.in. Fax: 91-80-3348535 or 91-80-3341683.

‡ Indian Institute of Science.

§ School of Environmental Sciences.

|| School of Life Sciences.

⊗ Abstract published in *Advance ACS Abstracts,* August 15, 1997.

[1] Abbreviations: *E. histolytica*, *Entamoeba histolytica*; *E. coli*, *Escherichia coli*; CaBP, calcium binding protein; MOPS, (3-[*N*-morhpholino]propanesulfonic acid); 5,5′ Br2 BAPTA, Glycine, *N,N*′-[1,2-ethanediylbis[oxy(4-bromo-2,1-phenylene)]]bis[*N*-[2-[(acetyloxy)-methoxy]-2-oxoethyl]-, bis[(acetyloxy)methyl] ester; GdnHCl, guanidine hydrochloride; CNBr, cynogen bromide.

S0006-2960(97)00254-7 CCC: $14.00

Site	position	1	2	3	4	5	6	7	8	9	10	11	12
		*		*		*		*		*			*
CaBP(*E.hist*)	Site 1	D	V	N	G	D	G	A	V	S	Y	E	E
	Site 2	D	A	D	G	N	G	E	I	D	Q	N	E
	Site 3	D	V	D	G	D	G	K	L	T	K	E	E
	Site 4	D	A	N	G	D	G	Y	I	T	L	E	E
Calmodulin	Site 1	D	K	D	G	D	G	E	V	S	F	E	E
	Site 2	D	K	D	G	N	G	T	I	T	T	K	E
	Site 3	D	K	D	G	N	G	Y	I	S	A	A	E
	Site 4	N	I	D	G	D	G	E	V	N	Y	E	E
Troponin C	Site 1	D	A	D	G	G	G	D	I	S	T	K	E
	Site 2	D	E	D	G	S	G	T	I	D	F	E	E
	Site 3	D	K	N	A	N	G	F	I	D	I	E	E
	Site 4	D	K	N	N	N	G	R	I	D	F	D	E
Parvalbumin	Site 1	D	Q	D	K	S	G	F	I	E	E	D	E
	Site 2	D	S	D	G	D	G	K	I	G	V	D	E

FIGURE 1: The sequences of the calcium binding sites of CaBP are compared with the EF loops of calmodulin, troponin C and parvalbumin. Ligand coordinators crystallographically determined/derived from sequence homology are marked by the asterisk (∗).

indicate the presence of one high-affinity Ca-Mg site, one high-affinity Ca-specific site and two low-affinity Ca-specific sites. Calcium and magnesium titrations were also performed on a cleaved peptide fragment containing the N-terminal domain so as to enable the assignment of sites to the two domains. DSC measurements could not be performed on this protein as we were unable to get the fully unfolded baseline even at a temperature of 120 °C. Here we present our attempt to study the nature of the unfolding of the two domains using the denaturant GdnHCl, by conducting Ca^{2+}/Mg^{2+} titrations in the presence of various concentrations of GdnHCl.

The thermodynamics and cooperativity of the binding of Ca^{2+} and Mg^{2+} to CaBP were determined in terms of the binding constants (K_{bi}) and changes in the free energy ($\Delta G_{bi}°$), entropy ($\Delta S_{bi}°$), and heat capacity (ΔC_p), for the following reactions:

$$\mathrm{CaBP} + \mathrm{X} \leftrightarrow \mathrm{CaBP{\cdot}X}$$

where X represents the Ca^{2+} or Mg^{2+} ion concentration and

$$K_{b1} = [\mathrm{CaBP{\cdot}X}]/[\mathrm{CaBP}][\mathrm{X}]$$

$$\text{and } \mathrm{CaBP{\cdot}X} + \mathrm{X} \leftrightarrow \mathrm{CaBP{\cdot}X_2}$$

$$\text{where } K_{b2} = [\mathrm{CaBP{\cdot}X_2}]/[\mathrm{CaBP{\cdot}X}][\mathrm{X}]$$

$$\text{Similarly } K_{b3} = [\mathrm{CaBP{\cdot}X_3}]/[\mathrm{CaBP{\cdot}X_2}][\mathrm{X}]$$

$$\text{and } K_{b4} = [\mathrm{CaBP{\cdot}X_4}]/[\mathrm{CaBP{\cdot}X_3}][\mathrm{X}] \quad (1)$$

These thermodynamic parameters were determined as a function of temperature from ITC measurements. We have used the *E. histolytica* CaBP as a paradigm to illustrate the use of isothermal titration calorimetry to deduce information on the hierarchy of the ion binding sites and to utilize the ion binding parameters to probe protein unfolding as a function of denaturant concentration.

EXPERIMENTAL PROCEDURES

Materials. The plasmid encoding the gene for CaBP was expressed in *E. coli* strain BL21(DE3)pLysS. The procedure for the purification of CaBP has been described previously (Prasad et al., 1993). All the experiments utilized 20 mM MOPS buffer adjusted to pH 7.0 and passed through a CHELEX 100 column to make the buffer metal ion free. All solutions were passed through 0.22 μm Corning filters and degassed before use. The concentrations of the GdnHCl stock solutions were determined by refractive index measurements (Pace et al., 1989) on an Abbe refractometer. Residual metal ion content in metal ion free protein and buffers was made using a fluorescent BAPTA calcium sensitive dye. The purity of the protein was checked on a preparative C18 HPLC column and by tricine SDS electrophoresis. A protein analysis was performed by comparing the optical densities at 562 nm of samples of the solution to those of bovine serum albumin solutions after adding 4% $CuSO_4$ and bicinchoninic acid reagent to the samples. The concentrations were determined by UV absorption spectroscopy using an extinction coefficient of $\epsilon^{280} = 5120\ M^{-1}\ cm^{-1}$. The ligand solutions were made by dissolving calcium or magnesium chloride in the final dialysate solution so that the ligand solvent was the same as the protein solvent. The cleaved peptide containing the N-terminal fragment was obtained by a CNBr digestion of the native protein in 70% formic acid for 18 h at room temperature. The cleaved peptide was purified by reverse phase HPLC using a preparative C18 column (Waters) . All the reagents used were of analytical grade from Sigma. 5,5′-Br_2BAPTA was obtained from Molecular Probes, Inc. GdnHCl used was the Ultrapure grade obtained from Gibco BRL.

CD Measurements and Gdn-HCl-Induced Denaturation. CD measurements were carried out on a Jasco J500 spectropolarimeter attached to a DP-501N data processor. Equilibrium unfolding as a function of GdnHCl concentration was monitored by far- as well as near-UV CD. Spectra were collected at a scan speed of 10 nm/min and a response time of 8 s. Each spectrum was an average of at least eight scans. Secondary structure was monitored at 222 nm at a protein concentration of 16 μM using a cuvette of path length 0.1 cm. Near-UV CD measurements were recorded at 276 nm using a 0.5 cm path length cuvette at a protein concentration of 80 μM. The sample temperature was maintained using a Julabo circulating water bath.

ITC Measurements. The titration calorimetry measurements were performed with a Microcal Omega titration calorimeter as described earlier (Wiseman et al., 1989; Schwarz et al.,1991). Samples were centrifuged prior to the titration and were examined for precipitates, if any, after the titration. No precipitate was observed even at the lowest ionic strength of 1 mM MOPS. A typical titration consisted of injecting 5−10 μL aliquots of 10 mM ligand solutions into 0.08−0.32 mM of the protein solution after every 3.5 min to ensure that the titration peak returned to the baseline prior to the next injection. Aliquots of more concentrated ligand solutions were injected into just the dialysate solutions in separate ITC runs in order to measure the heats of dilutions of the ligand. No heat of dilutions was observed even at a ligand concentration of 20 mM.

Fluorescence Measurements. The tirations of Ca^{2+} with apo-CaBP were carried out on a Jasco FP-777 spectrofluo-

rometer at a protein concentration of 35 μM employing intrinsic tyrosine fluorescence. The exitation was at 275nm with the slit width set to 1.5 nm and the emission was recorded at 305 nm with the slit width set to 5nm. Each reading was an average over 4 cycles, with the response time set to 1 min.

Competitive Binding Measurements Using 5,5′-Br$_2$-BAPTA. The absorbance changes observed upon the binding of the chromophoric chelator 5,5′-Br$_2$ BAPTA to Ca^{2+} were recorded on a Jasco Model 7850 UV/VIS spectrophotometer following the methodology as reported earlier (Linse et al., 1990), at protein and BAPTA concentrations in the range 25−30 μM.

ITC Data Analysis. For an analysis of the scans which exhibited a continuous monotonic decrease in the titration peak with the addition of titrant, the first data fitting was made assuming a single set of identical sites where Q_t, is related to the total ligand concentration, $[X]_t$, via the following equation (Wiseman et al., 1989):

$$Q_t = n[\mathrm{CaBP}]_t\Delta H_b V(1 + [X]_t/n[\mathrm{CaBP}]_t + 1/nK_b[\mathrm{CaBP}]_t - [(1 + [X]_t/n[\mathrm{CaBP}]_t + 1/nK_b[\mathrm{CaBP}]_t) - 4[L]_t/n[\mathrm{CaBP}]_t]^{1/2}]/2 \quad (2)$$

where Q_t is the total heat content of the solution contained in volume V, n is the stoichiometry, K_b is an intrinsic binding constant, ΔH_b is an intrinsic heat of binding, $[\mathrm{CaBP}]_t$ is the total site concentration, and V is the cell volume. The value of Q_t above can be calculated at the end of the ith injection and designated Q_i. The change in the heat content from the completion of the $i - 1$ injection to the completion of the ith injection is calculated after a correction for the displaced volume. The expression for Q_t in eq 2 applies only to the liquid contained in a constant volume V. As some of the liquid in V after the $i - 1$ injection will no longer be in V after the ith injection (dV_i = injection volume) even though it will contribute to the heat effect before it passes out of the working volume V, the expression for the heat released Q_i from the ith injection gets modified as (Yang et al., 1990)- where dV_i represents the volume of titrant added. Each

$$\Delta Q_i = Q_i + dV_i/2V[Q_i + Q_{i-1}] - Q_{i-1} \quad (3)$$

titration calorimetry scan yeilds values for n, ΔH_b and, since the site concentration is used, the intrinsic binding constant K_b. These values were then used to fit the complex titration curves for the titration of calcium ions with CaBP with a model for interacting sites. Since the concentrations of all liganded species [CaBP·X$_i$] can be expressed in terms of the nonliganded species, [CaBP], the fraction of total macromolecule bound, F_is are given by

$$F_0 = 1/P$$
$$F_1 = K_1[X]/P$$
$$F_2 = K_1K_2[X]^2/P$$
$$\downarrow$$
$$F_4 = K_1K_2K_3K_4[X]^4/P \quad (4)$$

where $P = 1 + K_1[X] + K_1K_2[X]^2 + \ldots + K_1K_2K_3K_4[X]^4$ and $X_t = [X] + [\mathrm{CaBP}]_t\sum iF_i$ (5)

Once K_1-K_4 were assigned, eq 6 was solved for [X] and the F_is were then calculated from eq 5 and the heat content after the ith injection is then given by

$$Q = [\mathrm{CaBP}]_tV_0(F_1\Delta H_1 + F_2[\Delta H_1 + \Delta H_2] + \ldots + F_4[\Delta H_1 + \Delta H_4]) \quad (6)$$

The heat released per addition of titrant is then fitted to eq 3 using the eight parameters K_{bi}s and H_{bi}s, where ΔH_{bi}s are the enthalpy changes of binding between the four binding reactions (eq 1). The individual binding constants thus obtained using the sequential model are macroscopic terms containing contributions from multiple binding sites. Values for $\Delta G_b°$ and $\Delta S_b°$ were determined from the fundamental equations of thermodynamics:

$$\Delta G_{bi}° = -RT\ln(K_{bi}) = \Delta H_{bi} - T\Delta S_{bi}° \quad (7)$$

where $R = 8.3144$ J K^{-1} mol^{-1} and T is the absolute temperature. Cooperativity between two sites in either globular domain of the molecule can be characterized by $\Delta\Delta G$, the effect of Ca^{2+} binding to one of the sites on the free energy of Ca^{2+} binding to the other site (Weber, 1975; Linse et al., 1990) which is determined as

$$\Delta\Delta G = \Delta G_{I,II} - \Delta G_I = \Delta G_{II,I} - \Delta G_{II} = -RT\ln(K_{I,II}/K_I) = -RT\ln(K_{II,I}/K_{II}) \quad (8)$$

where $\Delta G_{I,II}$ is the free energy of Ca^{2+} binding to site I when a Ca^{2+} ion is bound to site II, and $K_{I,II}$ is the corresponding microscopic site binding constants. We then use the relations between the macroscopic and the microscopic binding constants

$$K_1 = K_I + K_{II} \text{ and } K_1K_2 = K_IK_{II,I} = K_{II}K_{I,II}$$

$$\text{Thus } -\Delta\Delta G = RT\ln(4K_2/K_1) + RT\ln((\eta + 1)^2/4\eta) \quad (9)$$

where $\eta = K_{II}/K_I$. The second term is zero for $\eta = 1$ (equally strong sites), and thus one obtains the lower limit on $-\Delta\Delta G$ solely from the macroscopic binding constants as

$$-\Delta\Delta G_{\eta=1} = RT\ln(4K_2/K_1) \quad (10)$$

RESULTS

As in the case of the other CaBP's, binding of Ca^{2+} induces large conformational changes in this CaBP as well, as is evident from the far- and near-UV CD spectra (Figures 2 and 3). Another property that this protein shares with some of the calmodulins is its high thermal stability. GdnHCl-induced denaturation experiments, carried out using spectroscopic probes like circular dichroism and fluorescence indicate that this protein, in its apo form, loses its tertiary structure substantially or almost totally at about 2.5 M GdnHCl concentration, whereas its secondary structure persists up to 6.0 M GdnHCl, highlighting the complexity in its unfolding behavior (Figure 7). This suggests that one of the two domains of CaBP may unfold earlier than the other. Earlier studies on troponin C using DSC (Ingraham et al., 1982) assign a higher temperature transition for unfolding to the N-terminal portion of the molecule, which contains the calcium-specific sites which have low affinity for calcium and of a lower temperature transition to the

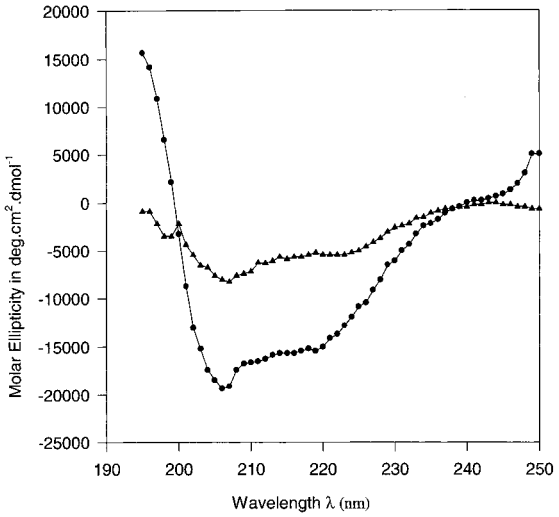

FIGURE 2: Far-UV spectra of apo (▲) and holo (●) CaBP at pH 7.0, 20 °C. The value of Θ_{222} is −5434.78 deg cm^2 dmol^{-1} for apo and −14130.43 deg cm^2 dmol^{-1} for the holo form.

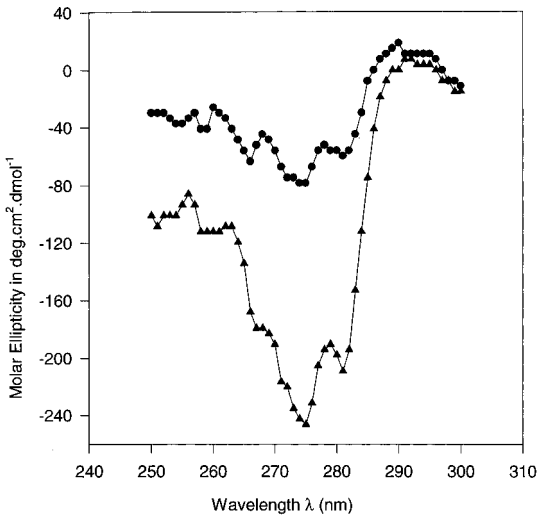

FIGURE 3: Near-UV spectra of apo (●) and holo (▲) CaBP at pH 7.0, 20 °C . The value of Θ_{276} is −78.358 deg cm^2 dmol^{-1} for apo and −242.537 deg cm^2 dmol^{-1} for the holo form.

unfolding of the C-terminal portion which contains the high-affinity Ca-Mg sites.

A typical calorimetric reaction of the addition of aliquots of Ca^{2+} ligand to CaBP is shown in Figure 4a along with its ΔQ *vs* $[X]_t/[CaBP]_t$ in Figure 5b. Analysis of the data represented in Figure 4b using eqs 2−6 indicates that the reactions represented in eq 1 have the following characteristics: there exist four sites which bind calcium, two sites of low affinity and two sites of high affinity. Both pairs of sites show positively cooperative interaction. One of the high-affinity sites is endothermic, while the other one is exothermic. Both of the low-affinity sites are exothermic in nature. The thermodynamic parameters corroponding to these binding reactions are listed in Table 1. A representative titration of Ca^{2+} to CaBP employing intrinsic tyrosine fluorescence is shown in Figure 6a and the corrsponding Hill's plot is shown in Figure 6b. Application of Br_2 BAPTA as an indicator ligand for calcium binding and results obtained by the fluorescence measurements also suggest that CaBP has four sites with K_b values that are in agreement with those obtained by the titration calorimetric data for at least three sites. Incorporation of the binding constants as

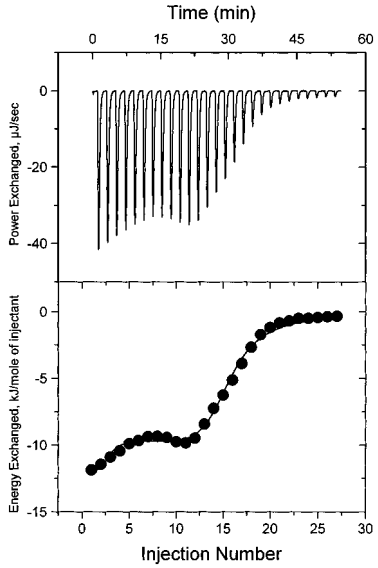

FIGURE 4: (a) A calorimetric titration of 6.7 μL aliquots of 10 mM $CaCl_2$ into 0.20 mM of apo CaBP in 20 mM MOPS buffer at 19 °C. (b) The heat exchanged per mole of titrant versus the ratio of the total concentration of ligand to the total concentration of protein and the best least-squares fit of the data to eqs 2−7 of the text.

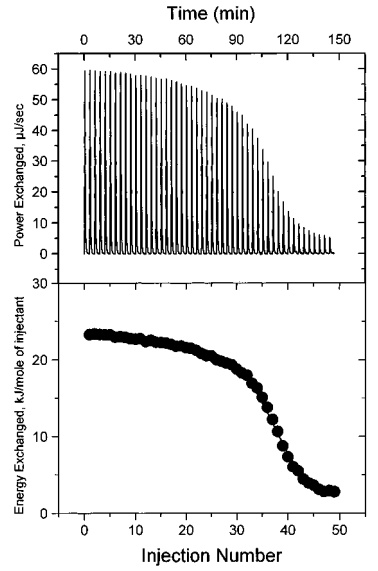

FIGURE 5: (a) A calorimetric titration of 8 μL aliquots of 10 mM $MgCl_2$ into 0.32 mM of apo CaBP in 20 mM MOPS buffer at 20 °C. (b) The heat exchanged per mole of titrant versus the ratio of the total concentration of the ligand to the total concentration of protein and the best least-squares fit of the data.

obtained from the spectroscopic data in the ITC data analysis give the values if the four K_{bi}s and H_is, that are quite similar to the values obtained using the *ab initio* fits, with the sequential model for the ITC data, thus validating the fitting procedure used for the analysis of the calorimetric data. The calculated $\Delta\Delta G$ values for the cooperativity between two sites, of either lower or higher affinity, are shown in Table 2. Each parameter for all the binding reactions (Table 1) is an average of at least two to three different titration runs using several different protein and ligand concentrations. As seen in Table 2, both pairs of sites show positive cooperativity, with the high-affinity sites (C-terminal domain in analogy to other CaBP's) showing 5-fold higher cooperativity than the low-affinity (N-terminal domain) sites. However, in the case of Ca^{2+} titrations performed on CaBP saturated

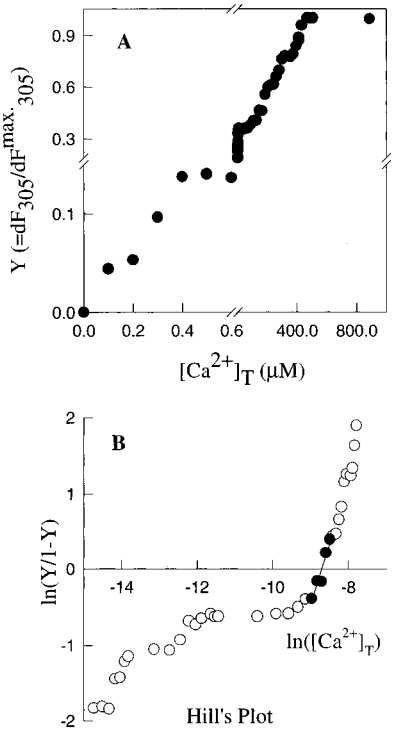

FIGURE 6: (a) A fluorescence titration of 1 μL aliquots of 0.001−100 mM $CaCl_2$ into 45 μM of apo CaBP in 20 mM MOPS buffer at 20 °C. (b) The Hill's plot for the fluorescence titration which gives a Hill's coefficient of 1.82.

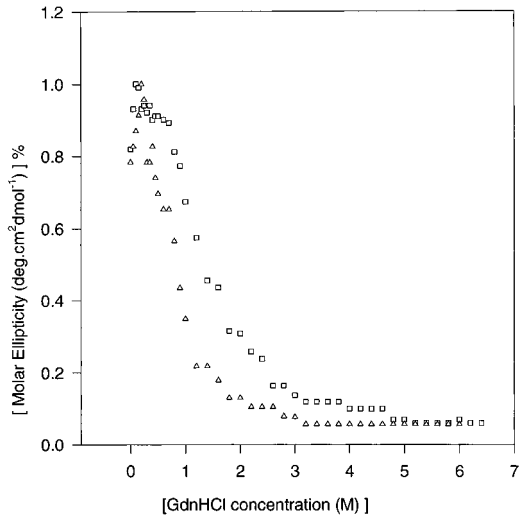

FIGURE 7: Equlibrium denaturation curves of apo CaBP at 20 °C, pH 7.0. GdnHCl-induced denaturation was followed by monitoring mean residue ellipticity at 222 nm (□) for the secondary structure and 276 nm (△) for the tertiary structure.

with Mg^{2+}, the cooperativity reverses sign, and both pairs of sites now exhibit negative cooperativity with magnitudes similar to those of native CaBP. Titrations performed on the cleaved N-terminal fragment show the presence of two Ca^{2+}-specific sites with positive cooperative interaction between them. The binding affinities, however, are higher than the native (Table 2). The binding reaction of Mg^{2+} with CaBP is shown in Figure 5a, with its corrosponding ΔQ_i *vs* $[X]_t/[CaBP]_t$ in Figure 5b. This could only be fitted to a one-site model . In the case of Ca^{2+} titrations performed on the native protein in the presence of varying amounts of KCl, the binding affinities and enthalpies show pronounced effects of ionic strength as is to be expected (Table 3). These titrations, however, can still be examined by the four-site model.

Concentrations of GdnHCl corresponding to specfic points on the unfolding curve shown in Figure 7 were selected for the examination of the binding reactions. Up to a concentration of 0.2 M, the binding pattern of CaBP to Ca^{2+} or Mg^{2+} appears to be the same as that of the native protein. At a concentration of 0.25 M GdnHCl, the interacting four site model could no longer be fitted to the calorimetric reaction shown in Figure 8a. The data indeed fits well to the two-site model, with both the sites showing high binding affinity and negligible cooperativity (Table 4). A similar pattern for reaction heats was observed upto a GdnHCl concentration of 2.5 M. Above 2.5 M GdnHCl concentration, however, the fitting of the data to a suitable model became difficult, primarily due to the drastic reduction in the binding affinities. At a GdnHCl concentration of 6.5 M, only the baseline pattern was obtained, indicating that no binding occurs at this concentration.

DISCUSSION

The process by which Ca^{2+} binding to calmodulin induces large conformational changes is now being understood by an examination of the Calmodulin structure in its apo and holo forms (Kuboniwa et al., 1991; Babu et al., 1988; Herzberg et al., 1988, Zhang et al.,1995; Gagne et al., 1995). These conformational changes have been reported to be important for calmodulin to bind to its effector proteins and trigger the next reaction in the Ca^{2+} signaling pathway. The functional differences in this family of proteins is supposed to arise from the differential tuning of ion binding characteristics, namely its ion binding affinity, specificity, cooperativity, and kinetics. These parameters define either the Ca^{2+} activation threshold of a regulatory protein or the capacity of a buffer protein to sequester calcium (Falke et al., 1994). The ion binding affinities, specificities, and the cooperative nature of binding indicates that *E. histolytica* CaBP could function as a trigger protein. Also of interest in this context are the differences in the nature of the cooperative interactions between the sites in the two domains. It has been shown earlier (Waltersson et al., 1993) that mutations made at residue position 3 (an aspartate residue in all the four sites of calmodulin, Figure 1), have opposite effects on the cooperativity in the N- and C-terminal domains. When mutated to asparagine at binding sites 2 and 3 of calmodulin, the cooperativity in the N-terminal domain is increased while it decreases the cooperativity in the C-terminal domain. In the case of CaBP, asparagine residues occur at position 3 in sites 1 and 4. We, however, observe that these substitutions result in higher cooperativity in the C-terminal domain and lower cooperativity in the N-terminal domain. In order to confirm the assignment of the N-terminal domain to the Ca^{2+}-specific sites and the C-terminal domain to the Ca-Mg sites, we performed Ca^{2+} and Mg^{2+} titrations on a cleaved N-terminal fragment containing two sites and the central linker. This N-terminal domain fragment shows the presence of two Ca^{2+}-specific sites with positive cooperative interaction comparable to the native protein. The binding affinities suggest the possibility of interdomain cooperativity, that is, the down regulation of the calcium binding affinity of the N-terminal domain by the C-terminal domain. This inference could be ambiguous given the fact that the fragment contains the central linker

Table 1: Thermodynamic Parameters of Ca^{2+} and Mg^{2+} Binding to CaBP at pH 7.0 in 20 mM MOPS Buffer[a]

ligand	site	T (°C)	K_b (M^{-1})	ΔH	$\Delta G°$ (kJmol^{-1})	$T\Delta S°$
Ca^{2+}	I	19	$(4.98 \pm 1.2) \times 10^3$ $((1.2 \pm 0.3) \times 10^3)$ $[(1.52 \pm 1.4) \times 10^2]$	-13.09 ± 0.87	-20.66 ± 0.21	6.857 ± 0.9
	II		$(3.13 \pm 0.41) \times 10^3$ $((3.76 \pm 0.4) \times 10^3)$ $[(5.1 \pm 1.3) \times 10^4]$	-47.69 ± 5.46	-19.53 ± 0.12	-28.16 ± 5.46
	III		$(1.03 \pm 0.19) \times 10^4$ $((7.9 \pm 1.6) \times 10^4)$ $[(8.98 \pm 1.5) \times 10^4)$	117.57 ± 20.08	-22.43 ± 0.16	140.0 ± 12.1
	IV		$(1.66 \pm 0.1) \times 10^5$ $((1.3 \pm 0.4) \times 10^5)$ $[(1.8 \pm 0.3) \times 10^5]$	-116.31 ± 10.46	-29.17 ± 0.08	-87.14 ± 10.46
Ca^{2+}	I	20	$(3.7 \pm 0.38) \times 10^4$	$-21.4\,2 \pm 0.16$	-25.53 ± 0.1	4.121 ± 0.19
(Mg^2 saturated)	II		$(4.3 \pm 0.45) \times 10^2$	-102.98 ± 19.27	-14.723 ± 0.1	-88.26 ± 8.3
	III		$(4.7 \pm 0.48) \times 10^5$	47.45 ± 19.27	-31.706 ± 0.01	79.16 ± 6.27
	IV		$(1.07 \pm 0.86) \times 10^3$	-24.22 ± 2.29	-16.9 ± 0.8	-7.284 ± 2.3
Ca^{2+}	I	20	$(1.8 \pm 0.4) \times 10^7$	-36.88 ± 0.75	-40.69 ± 0.22	3.81 ± 0.78
(N-terminal Domain)	II		$(3.5 \pm 0.5) \times 10^5$	-62.65 ± 0.75	-31.09 ± 0.14	-31.56 ± 0.77
Mg^{2+}	III	20	$(3.61 \pm 0.29) \times 10^4$	23.17 ± 0.16	-25.54 ± 0.08	2.38 ± 0.18

[a] The K_b values obtained by the fluorescence method and by the competitive binding expreiment with 5,5′ Br_2 BAPTA are given in the parentheses and brackets, respectively.

Table 2: Free Energy of the Binding of the First Two ($\Delta G^{12}_{tot} = -RT \ln(K_1K_2)$) and Last Two ($\Delta G^{34}_{tot} = -RT \ln(K_3K_4)$) Ca^{2+} Ions to CaBP and a Lower Limit of Cooperativity within Each Pair ($-\Delta\Delta G^{12}_{\eta=1} = RT \ln(4K_2/K_1)$ and $-\Delta\Delta G^{34}_{\eta=1} = RT \ln(4K_4/K_3)$)

titration type	ΔG^{12}tot (kJmol^{-1})	$-\Delta\Delta G^{12}_{\eta=1}$ (kJmol^{-1})	ΔG^{34}_{tot} (kJmol^{-1})	$-\Delta\Delta G^{34}_{\eta=1}$ (kJmol^{-1})
Ca^{2+}	-40.34 ± 0.25	2.24	-51.79 ± 0.2	10.15
Ca^{2+} (Mg2+ saturated)	-40.39 ± 0.3	-1.86	-48.81 ± 0.25	-11.44
Ca^{2+} (N-terminal Domain)	-77.40 ± 0.38	0.61		
Ca^{2+} in 0.05 M KCl	-34.54 ± 0.34	9.93	-32.72 ± 0.35	14.47
Ca^{2+} in 0.1 M KCl	-34.90 ± 0.39	8.76	-55.24 ± 3.38	13.51
Ca^{2+} in 0.15 M KCl	-36.41 ± 0.36	11.36	-55.83 ± 4.2	14.13
Ca^{2+} in 0.25 M KCl	-35.54 ± 0.35	10.71	-53.90 ± 3.9	15.27
Ca^{2+} in 0.25 M GdnHCl			-64.89 ± 5.2	2.17
Ca^{2+} in 0.5 M GdnHCl			-62.47 ± 4.8	1.47
Ca^{2+} in 0.75 M GdnHCl			-69.67 ± 4.6	0.23
Ca^{2+} in 1 M GdnHCl			-58.14 ± 5.1	0.29
Ca^{2+} in 1.75 M GdnHCl			-54.99 ± 5.4	-0.34
Ca^{2+} in 2.5 M GdnHCl			-57.19 ± 5.2	0.54

Table 3: Thermodynamic Parameters of Calcium Binding to CaBP in 20 mM MOPS + KCl

ligand	site	T (°C)	K_b (M^{-1})	ΔH	$\Delta G°$ (kJ/mol^{-1})	$T\Delta S°$
Ca^{2+} in 0.05 M KCl	I	20	$(3.13 \pm 0.4) \times 10^2$	-57.79 ± 8.78	-13.99 ± 0.12	-43.8 ± 47.78
	II		$(4.614 \pm 0.8) \times 10^3$	-593.2 ± 52.29	-20.55 ± 0.17	-572.65 ± 52.8
	III		$(7.098 \pm 1.2) \times 10^2$	2578.18 ± 112.8	-15.99 ± 0.16	2594.17 ± 113
	IV		$(6.75 \pm 0.9) \times 10^5$	-2141.31 ± 181.9	-32.69 ± 0.13	-2108.7 ± 182.1
Ca^{2+} in 0.1 M KCl	I	20	$(4.28 \pm 1.36) \times 10^2$	-50.84 ± 6.35	-14.76 ± 0.31	-36.08 ± 6.35
	II		$(3.9 \pm 0.9) \times 10^3$	-571.16 ± 71.47	-20.14 ± 0.23	-551.02 ± 71.7
	III		$(1.04 \pm 0.24) \times 10^4$	2054.82 ± 163.1	-22.53 ± 0.23	2077.35 ± 163
	IV		$(6.72 \pm 1.09) \times 10^5$	-1633.14 ± 97.27	-32.76 ± 0.16	-1600.38 ± 101.9
Ca^{2+} in 0.15 M KCl	I	20	$(3.42 \pm 1.11) \times 10^2$	-42.93 ± 6.19	-14.21 ± 0.32	-28.72 ± 6.2
	II		$(9.04 \pm 1.13) \times 10^3$	-466.59 ± 40.67	-22.19 ± 0.35	-444.4 ± 43.7
	III		$(1.04 \pm 0.37) \times 10^4$	1817.78 ± 96.0	-22.53 ± 0.36	1840.31 ± 98
	IV		$(8.61 \pm 2.5) \times 10^5$	-1499.54 ± 108.5	-33.29 ± 0.3	-1466.25 ± 112
Ca^{2+} in 0.25 M KCl	I	20	$(3.27 \pm 0.55) \times 10^2$	-57.85 ± 4.64	-14.1 ± 0.17	$-43.7\,5 \pm 5.1$
	II		$(6.62 \pm 1.01) \times 10^3$	-401.54 ± 44.94	-21.43 ± 0.15	-380.11 ± 49
	III		$(5.55 \pm 1.21) \times 10^4$	2219.52 ± 206.0	-26.61 ± 0.22	2246.13 ± 210.5
	IV		$(7.32 \pm 1.4) \times 10^5$	-1958.21 ± 185.0	-32.89 ± 0.2	-1925.32 ± 192

whose contribution towards interdomain cooperativity has not been determined. We, however, observe that this domain shows very little structural change upon addition of Ca^{2+} as observed by far UV CD spectroscopy, which is in contrast with the native protein Figure 2.

In this study, we have used the ion binding parameters to monitor domain unfolding. The transition of the calorimetric binding pattern from four interacting sites to two sites of higher affinity with weakly positive cooperative interaction even at as low a concentration of GdnHCl as 0.25 M, shows that the sites of lower affinity to Ca^{2+} are disabled preferentially over their high-affinity counterparts (Figure 8b) . The far- and near-UV CD spectra (Figure 7) suggest that GdnHCl concentrations up to 1 M could play a stabilizing role as seen by the burst in the molar ellipticity values. This initial stabilization has been attributed to the formation of stable transition intermediates (Matthews, 1993; Fersht, 1993; Ptitsyn et al., 1993). These studies show that the formation of stable transition intermediates may not necessarily be correlated with the generation of the optimal functional or

Table 4: Thermodynamic Parameters of Calcium Binding to CaBP in 20 mM MOPS + GdnHCl

ligand	site	T (°C)	K_b (M^{-1})	ΔH	$\Delta G°$ (kJ mol^{-1})	$T\Delta S°$
Ca^{2+} in 0.25 M GdnHCl	III	20	$(1.9 \pm 0.29) \times 10^6$	-25.84 ± 0.49	-35.21 ± 0.15	9.363 ± 0.51
	IV		$(1.95 \pm 0.1) \times 10^5$	-14.57 ± 0.42	-29.67 ± 0.05	15.1 ± 0.424
0.5 M GdnHCl	III	20	$(1 \pm 0.14) \times 10^6$	-31.01 ± 0.75	-33.65 ± 0.14	2.64 ± 0.76
	IV		$(1.37 \pm 0.1) \times 10^5$	-12.59 ± 0.89	-28.82 ± 0.07	16.19 ± 0.9
0.75 M GdnHCl	III	20	$(3.1 \pm 1) \times 10^6$	-35.48 ± 2.03	-36.41 ± 0.32	-0.93 ± 2.06
	IV		$(8.5 \pm 0.26) \times 10^5$	-10.45 ± 1.45	-33.25 ± 0.03	22.8 ± 1.45
1 M GdnHCl	III	20	$(3.23 \pm 0.75) \times 10^5$	-38.49 ± 3.76	-30.82 ± 0.23	-7.67 ± 3.77
	IV		$(7.18 \pm 0.63) \times 10^4$	-10.79 ± 2.16	-33.25 ± 0.08	22.8 ± 2.16
1.75 M GdnHCl	III	20	$(1.72 \pm 0.96) \times 10^5$	-41.89 ± 4.64	-29.36 ± 0.55	-12.53 ± 4.67
	IV		$(3.7 \pm 0.10) \times 10^4$	-9.974 ± 0.9	-25.624 ± 0.02	25.53 ± 0.9
2.5 M GdnHCl	III	20	$(2.8 \pm 1.042) \times 10^4$	-29.83 ± 4.46	-30.55 ± 0.37	-0.72 ± 4.48
	IV		$(5.61 \pm 1.62) \times 10^4$	-2.52 ± 2.62	-26.61 ± 0.3	24.08 ± 2.64

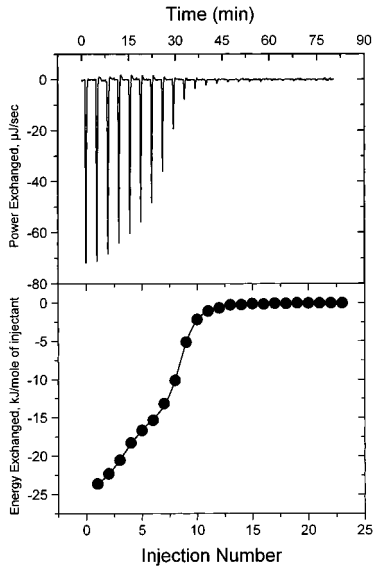

FIGURE 8: (a) A calorimetric titration of 6.7 μL aliquots of 10 mM $CaCl_2$ into 0.28 mM of apo CaBP in 20 mM MOPS buffer containing 0.025 M GdnHCl at 20 °C. (b) The heat exchanged per mole of titrant versus the ratio of the total concentration of the ligand to the total concentration of the protein and the best least-squares fit of the data into the two-site model.

the binding conformer of the protein. Notwithstanding the likely reasons for the above dichotomy observed between the overall stabilization of the protein and its ligand binding ability, the inability of the low affinity sites to bind Ca^{2+} suggests that the N-terminal domain is affected first. These results are further corroborated by the fact that titrations performed at 60 °C, reveal further reduction in the affinities of the N-terminal sites. Similarly, we observe that both the sites in the C-terminal domain of the molecule become exothermic and the binding affinity for Mg^{2+} is lost. The inability of the Ca-Mg site to bind to Mg^{2+} in the presence of GdnHCl seems to suggest that the glutamate residue at position 12 of the ion binding loop (Figure 1, site III) may be unable to switch between the conformation needed to bind to Ca^{2+} (bidentate) to a monodentate mode preferred by Mg^{2+} (Falke et al., 1995).

In conclusion, we postulate that GdnHCl induces the domain containing the low-affinity site to unfold earlier than the domain containing the higher affinity sites. The high-affinity sites also get affected but nonetheless retain their ability to bind to Ca^{2+} with binding affinities comparable to the native protein at moderate to high denaturant concentrations. This observation is in contrast to the thermal unfolding reported earlier for troponin C (Ingraham et al.,1982), where the domain containing the higher affinity sites unfolds first. These results suggest that the N-terminal domain, which apparently is more compact, is the first to undergo destabilization and consequent unfolding.

ACKNOWLEDGMENT

We wish to thank Dr. R. Varadarajan for a critical reading of the manuscript and Mr. C. Ganesh for help in data analysis.

REFERENCES

Babu, Y. S., Bugg, C. E., & Cook, W. J. (1988) *J. Mol. Biol. 204*, 191−204.
Drabikowski, W., Brzeska, H., & Venyaminov, S. Y. (1982) *J. Biol. Chem. 257*, 11584−11590.
Falke, J. J., Drake, S. K., Hazard, A. L., Peersen, O. B. (1994) *Q. Rev. Biophys. 27*, 219−290.
Fersht, A. R. (1993) *FEBS Lett. 325*, 516.
Gagne, S. M., Tsuda, S., Li, M. X., Smillie, L. B., & Sykes, B. D. (1995) *Nat. Struct. Biol. 2* (9), 784−789.
Herzberg, O., & James, M. N. G. (1988) *J. Mol. Biol. 203*, 761−779.
Ingraham, R. H., & Swenson, C. A. (1983) *Eur. J. Biochem. 132*, 85−88.
Kuboniwa, H., Tjandra, N., Grzesiek, S., Ren, H., Klee, C. B., & Bax, A. (1995) *Nat. Struct. Biol. 2* (9), 768−776.
Masamoto, I., Tanokura, M., & Yamada, K. (1990) *J. Biochem. 107*, 127−132.
Matthews, C. R. (1993) *Annu. Rev. Biochem. 62*, 653−683.
Munoz, M., De, L., Moreno, M. A., Perez-Garcia, J. N., Tovar, J. R., & Hernandez, V. I. (1991) *Mol. Microbiol. 5*, 1701−1714.
Pace, C. N., Shirley, B, A., & Thomson J. A. (1989) in *Protein Structure: A Practical Approach* (Crieghton, T. E., Ed.) pp 311−330, IRL Press, Oxford, U.K.
Prasad, J., Bhattacharya, S. & Bhattacharya, A. (1993) *Cell Mol. Biol. Res. 39*, 167−175.
Ptitsyn, O. B. (1992) in *Protein Folding* (Crighton, T. E., Ed.) pp 243−300, W. H. Freeman, New York.
Ravdin, J. I., Murphy, C. F., Guerrant, R. L., Long-Kruz, S. A. (1985) *J. Inf. Dis. 152*, 542−549.
Sara, L., Helmersson, A., & Forsen, S. (1991) *J. Biol. Chem. 266*, 8050−8054.
Schwarz, F. P., Puri, K., & Surolia, A. (1991) *J. Biol. Chem. 266*, 24344−24350.
Waltersson, Y., Linse, S., Brodin, P., & Grundstrom, T. (1993) *Biochemistry 32*, 7866−7871.
Wang, C.-L. A. (1985) *Biochem. Biophys. Res. Commun. 130*, 426−430.
Wiseman, T., Williston, S., Brandts, J. F., Lin, L. N. (1989) *Anal. Biochem. 79*, 131−137.
Yang, C. P. (1990) *Omega Data in Origin*, pp 66, Microcal Inc., Northampton, MA.
Zhang, M., Tanaka, T., & Ikura, M. (1995) *Nat. Struct. Biol. 2*, *9*, 758−766.

BI9702546